7052–7065 *Nucleic Acids Research, 2020, Vol. 48, No. 13* *Published online 16 June 2020*
doi: 10.1093/nar/gkaa523

Rational design of antisense oligonucleotides modulating the activity of TLR7/8 agonists

Arwaf S. Alharbi [1,2,3,†], Aurélie J. Garcin [1,2,†], Kim A. Lennox [4], Solène Pradeloux [1,2], Christophe Wong [1,2], Sarah Straub [1,2,5,6], Roxane Valentin [1,2], Geneviève Pépin [1,2], Hong-Mei Li [1,2], Marcel F. Nold [7,8,9], Claudia A. Nold-Petry [7,8], Mark A. Behlke [4] and Michael P. Gantier [1,2,*]

[1]Centre for Innate Immunity and Infectious Diseases, Hudson Institute of Medical Research, Clayton, Victoria 3168, Australia, [2]Department of Molecular and Translational Science, Monash University, Clayton, Victoria 3800, Australia, [3]The Department of Clinical Laboratory Sciences, Faculty of Applied Medical Sciences, Taif University, Turabah 29179, Saudia Arabia, [4]Integrated DNA Technologies Inc., Coralville, IA 52241, USA, [5]Department of Microbiology and Immunology, The Doherty Institute for Infection and Immunity, The University of Melbourne, Parkville, Victoria 3010, Australia, [6]Institute of Innate Immunity, University Hospital Bonn, University of Bonn, Bonn 53127, Germany, [7]Ritchie Centre, Hudson Institute of Medical Research, Clayton, Victoria 3168, Australia, [8]Department of Paediatrics, Monash University, Clayton, Victoria 3168, Australia and [9]Monash Newborn, Monash Children's Hospital, Clayton, Victoria 3168, Australia

Received February 07, 2020; Revised June 04, 2020; Editorial Decision June 04, 2020; Accepted June 09, 2020

ABSTRACT

Oligonucleotide-based therapeutics have become a reality, and are set to transform management of many diseases. Nevertheless, the modulatory activities of these molecules on immune responses remain incompletely defined. Here, we show that gene targeting 2′-*O*-methyl (2′OMe) gapmer antisense oligonucleotides (ASOs) can have opposing activities on Toll-Like Receptors 7 and 8 (TLR7/8), leading to divergent suppression of TLR7 and activation of TLR8, in a sequence-dependent manner. Surprisingly, TLR8 potentiation by the gapmer ASOs was blunted by locked nucleic acid (LNA) and 2′-methoxyethyl (2′MOE) modifications. Through a screen of 192 2′OMe ASOs and sequence mutants, we characterized the structural and sequence determinants of these activities. Importantly, we identified core motifs preventing the immunosuppressive activities of 2′OMe ASOs on TLR7. Based on these observations, we designed oligonucleotides strongly potentiating TLR8 sensing of Resiquimod, which preserve TLR7 function, and promote strong activation of phagocytes and immune cells. We also provide proof-of-principle data that gene-targeting ASOs can be selected to synergize with TLR8 agonists currently under investigation as immunotherapies, and show that rational ASO selection can be used to prevent unintended immune suppression of TLR7. Taken together, our work characterizes the immunomodulatory effects of ASOs to advance their therapeutic development.

INTRODUCTION

With the recent approval of eight oligonucleotides-based therapeutics in the United States and European Union (1,2), and the prospect of many more to be commercialized from current phase III studies (3), therapeutic targeting of messenger RNA (mRNA) is set to play a large role in disease management in this decade. While different strategies have been developed to impact mRNA translation, such as recruiting RNase-H1 (with antisense oligonucleotides [ASOs] such as inotersen, or volanesorsen) or Ago2 (with small interfering RNAs [siRNAs] such as patisiran or givosiran) to actively degrade target mRNAs, or to promote splicing modulation (with ASOs such as eteplirsen and nusinersen), it is noteworthy that all therapeutic oligonucleotides approved to date rely on extensive chemical modifications. Such modifications are essential to prevent degradation by nucleases, and can also affect binding affinity to the target mRNA. These modifications can either be used to stabilise the phosphodiester (PO) internucleotide

*To whom correspondence should be addressed. Tel: +613 8572 2709; Fax: +613 9594 7114; Email: michael.gantier@hudson.org.au
†The authors wish it to be known that, in their opinion, the first two authors should be regarded as Joint First Authors.
Present address: Geneviève Pépin, Department of Medical Biology, Université du Québec à Trois-Rivières, Quebec G8Z 4M3, Canada.

© The Author(s) 2020. Published by Oxford University Press on behalf of Nucleic Acids Research.
This is an Open Access article distributed under the terms of the Creative Commons Attribution Non-Commercial License (http://creativecommons.org/licenses/by-nc/4.0/), which permits non-commercial re-use, distribution, and reproduction in any medium, provided the original work is properly cited. For commercial re-use, please contact journals.permissions@oup.com

linkages, as seen with the phosphorothioate (PS) backbone modification, or to stabilize the bases with sugar modifications (e.g. with 2′-*O*-methyl [2′OMe], 2′-methoxyethyl [2′MOE], 2′-fluoro [2′F] or locked nucleic acid [LNA]) (1).

In mammals, recognition of exogenous nucleic acids is a critical component of immune responses to pathogens and is achieved by a variety of innate immune sensors including, among others, the Toll-like-receptors (TLRs), such as TLR3, TLR7, TLR8 and TLR9, the retinoic acid-inducible gene-I (RIG-I)-like receptors, AIM2-like receptors, and the cyclic-GMP-AMP synthase (cGAS) pathway. It is therefore not surprising that select oligonucleotide therapeutics were found to instigate potent immune responses through direct engagement of such sensors (4–7), directing industry to closely consider and monitor such immune responses during pre-clinical and clinical development (8). Nevertheless, discrimination between self and non-self nucleic acids by innate immune sensors can be modulated by the presence of nucleic acid modifications rarely encountered in pathogens—as seen with 2′-*O*-methylated nucleosides that are 25 times more abundant in human ribosomal RNA than bacterial RNA (9). For example, TLR7 and TLR8 selectively detect RNA molecules and bases analogs (such as imidazoquinolines) and are inhibited by 2′OMe bases, facilitating molecular discrimination between self and non-self RNAs (9,10). As such, incorporation of select base modifications in therapeutic oligonucleotides, including 2′OMe, is a useful strategy to help mitigate aberrant immune responses by TLR7 and TLR8 (9,11), and is widely applied to therapeutic siRNAs (3).

However, this approach can also result in unintended immunosuppressive effects, as has been observed in the case of TLR7 and TLR8 antagonism by oligonucleotide sequences containing specific 2′OMe motifs (12). Similarly, PS-modified DNA oligonucleotides have been reported to antagonize sensing by TLR9 (13), TLR7 (14), AIM2 (15) and cGAS (16), in a sequence-dependent manner (17). Critically, given that most therapeutic oligonucleotides currently approved or under investigation combine PS and base modifications, whether such combinations impact the frequency of immunosuppression is not currently defined.

Here, while designing and testing RNase-H1-recruiting gapmer 2′OMe ASOs (with a central DNA core of 10 nt flanked by 5 nt of 2′OMe, on a PS backbone), we observed a divergent activity of the ASOs on TLR7 and TLR8 sensing of the low molecular weight synthetic ligand imidazoquinoline, Resiquimod (referred to as R848 hereafter), with most ASOs strongly inhibiting TLR7 but potentiating TLR8 sensing. We demonstrate that TLR7 inhibition by these gapmer ASOs can be attenuated by specific CUU-containing 2′OMe flanking regions. In addition, we show that the central DNA region of the 2′OMe gapmer ASOs plays an important role in enhancing TLR8 response to R848. Accordingly, we propose that rational selection of TLR8-potentiating ASOs could present new opportunities in the therapeutic development of bifunctional ASOs with gene-targeting and immunostimulatory activities.

MATERIALS AND METHODS

Ethics statement

Collection of peripheral blood mononuclear cells (PBMCs) from healthy donors was approved by Monash Health under the HREC reference 02052A.

Cell isolation, culture and stimulation

PBMCs were isolated from whole blood donations via density centrifugation using Histopaque-1770 (Sigma-Aldrich) as previously reported (18), and plated in RPMI 1640 plus L-glutamine medium (Thermo Fisher Scientific) complemented with 1× antibiotic/antimycotic and 10% heat-inactivated foetal bovine serum (referred to as complete RPMI). 293XL-hTLR8-HA (referred to as HEK-TLR8), 293XL-hTLR7-HA (referred to as HEK-TLR7) and 293XL-hTLR9-HA stably expressing TLR8, TLR7, and TLR9 respectively, were purchased from Invivogen, and were maintained in Dulbecco's modified Eagle's medium (Thermo Fisher Scientific) supplemented with 10% heat-inactivated foetal bovine serum (Thermo Fisher Scientific) and 1× antibiotic/antimycotic (Thermo Fisher Scientific) (referred to as complete DMEM) supplemented with 10 μg/ml Blasticidin (Invivogen). Parental wild-type (WT) THP-1, *UNC93B1*-deficient THP-1 (19) and matched clones reconstituted with fluorescent wild-type *UNC93B1* (20) were grown in complete RPMI. OCI-AML3 and MOLM13 were grown in RPMI supplemented with 20% heat inactivated foetal bovine serum and 1× antibiotic/antimycotic (their identity was confirmed by in house cell line identification service relying on PowerPlex HS16 System kit, Promega). All the cells were cultured at 37°C with 5% CO_2. Cell lines were passaged 2–3 times a week and tested for mycoplasma contamination on routine basis by PCR. For stimulations, THP-1, MOLM13 and OCI-AML3 were treated overnight with ASOs, prior to stimulation with 1 μg/ml R848 (Invivogen). HEK-TLR7 and HEK-TLR8 were treated with indicated concentration of ASOs for 20–50 min, prior to stimulation with R848, CL075, Gardiquimod (all from Invivogen) or 7-allyl-7,8-dihydro-8-oxoguanosine (Loxoribine – Sigma-Aldrich). All ASOs were synthesized by Integrated DNA Technologies (IDT), and resuspended in RNase-free TE buffer, pH 8.0 (Thermo Fisher Scientific). ASO sequences and modifications are provided in Supplementary Tables S1–S3. The cGAS ligand ISD70 (Supplementary Table S1) was prepared as previously described (21) and transfected with lipofectamine 2000 at 2.5 μg/ml final. The human TLR9 ligand known as Class B CpG oligonucleotide ODN 2006 was synthesized by IDT and resuspended in RNase-free TE buffer (Supplementary Table S1).

Luciferase assays

HEK293 cells stably expressing TLR7, 8 or 9 were transfected with pNF-κB-Luc4 reporter (Clontech), pLuc-IFN-β (a kind gift from K. Fitzgerald, University of Massachusetts) or pCCL5[RANTES]-Luc (a kind gift from G. Scholz, University of Melbourne) with Lipofectamine

2000 (Thermo Fisher Scientific), according to the manufacturer's protocol. Briefly, 500 000–700 000 cells were reverse-transfected with 400 ng of reporter with 1.2 μl of Lipofectamine 2000 per well of a six-well plate, and incubated for 3–24 h at 37°C with 5% CO_2. Following transfection, the cells were collected from the 6-wells and aliquoted into 96-wells, just before ASO and overnight TLR stimulation (as above described). The next day, the cells were lysed in 40 μl (for a 96-well plate) of 1X Glo Lysis buffer (Promega) for 10 min at room temperature. 15 μl of the lysate was then subjected to firefly luciferase assay using 40 μl of Luciferase Assay Reagent (Promega). Luminescence was quantified with a Fluostar OPTIMA (BMG LABTECH) luminometer.

Down-regulation of *HPRT* with ASOs in HeLa cells

For Figure 5A, each ASO was reverse-transfected in biological triplicate in 96-well plates by complexing the various ASO doses with 0.5 μl Lipofectamine 2000 (Thermo Fisher Scientific) in OptiMEM I (Thermo Fisher Scientific) for a total volume of 50 μl in each well. HeLa cells (20 000) were suspended in 100 μl DMEM supplemented with 10% FCS, added to the lipid-ASO complexes, then incubated for 24 h at 37°C and 5% CO_2. RNA was collected with the SV Total RNA Isolation Kit (Promega) with DNase1 treatment. cDNA was synthesized from ∼200 ng total RNA with anchored oligonucleotide dT and random hexamer primers (Integrated DNA Technologies) using SuperScript II Reverse Transcriptase (Thermo Fisher Scientific) as per the manufacturer's instructions. qPCR reactions were performed using ∼10 ng cDNA with Immolase DNA polymerase (Bioline), 500 nM of each primer and 250 nM probe in 10 μl reactions in 384-well plate format. Amplification reactions were run on an Applied Biosystems 7900HT (Thermo Fisher Scientific). All qPCR reactions were performed in triplicate for each sample and averaged. Linearized cloned amplicons were used as copy number standards to establish absolute quantitative measurements for each assay. *HPRT* (NM 000194) and *SFRS9* (NM 003769) expression levels were quantified by multiplexing 5′-nuclease assays, and *HPRT* levels normalized against *SFRS9*—used as internal reference control. Sequences of the primers and probe assays used are provided in Supplementary Table S1. Knock-down efficiency was calculated relative to NC1 and NC5 negative control ASOs.

Detection of cytokines

Human TNF-α and IP-10 were measured using BD OptEIA ELISA sets (BD Biosciences, #555212 and #550926, respectively), according to the manufacturers' instructions. Human IFN-α detection was carried out as previously reported (22). Tetramethylbenzidine substrate (Thermo Fisher Scientific) was used for quantification of the cytokines on a Fluostar OPTIMA (BMG LABTECH) plate-reader.

mRNA reverse transcription quantitative real-time PCR (RT-qPCR)

For Figures 4D and 5E, total RNA was purified from cells using the ISOLATE II RNA Mini Kit (Bioline). Random hexamer cDNA was synthesized from isolated RNA using the High-Capacity cDNA Archive kit (Thermo Fisher Scientific) according to the manufacturer's instructions. RT-qPCR was carried out with the Power SYBR Green Master Mix (Thermo Fisher Scientific) on the HT7900 and QuantStudio 6 RT-PCR system (Thermo Fisher Scientific). Each PCR was carried out in technical duplicate and human *18S* was used as reference gene. Each amplicon was gel-purified and used to generate a standard curve for the quantification of gene expression (used in each run). Melting curves were used in each run to confirm specificity of amplification. The primers used were the following: Human RSAD2: hRSAD2-RT-FWD TGGTGAGGTTCTGCAAAGTAG; hRSAD2-RT-REV GTCACAGGAGATAGCGAGAATG; hIFIT1: hIFIT1-FWD TCACCAGATAGGGCTTTGCT; hIFIT1-REV CACCTCAAATGTGGGCTTTT; h18S: h18S-FWD CGGCTACCACATCCAAGGAA; h18S-REV GCTGGAATTACCGCGGCT; hIFI44: hIFI44-FWD ATGGCAGTGACAACTCGTTTG; hIFI44: TCCTGGTAACTCTCTTCTGCATA; hIFNB: hIFNB1-FWD GCTTGGATTCCTACAAAGAAGCA; hIFNB1-REV: ATAGATGGTCAATGCGGCGTC; hHPRT-FWD: GACTTTGCTTTCCTTGGTCAG; hHPRT-REV GGCTTATATCCAACACTTCGTGGG; amplicons from RSAD2, IFIT1, and 18S PCRs were verified by Sanger sequencing. IFI44 and IFNB1 primers were from the Primer Bank (23), and HPRT primers were designed by IDT.

Statistical analyses

Statistical analyses were carried out using Prism 8 (GraphPad Software Inc.). Every experiment was carried out in biological triplicate (except Figures 2A, B, 4D and 5E, carried out in biological duplicate) and repeated a minimum of two independent times. One-way and two-way analyses of variance (ANOVA) were used when comparing groups of conditions, while two-tailed unpaired non-parametric Mann–Whitney *U* tests or unpaired two-tailed *t*-tests were used when comparing pairs of conditions. Symbols used: $*P \leq 0.05$, $**P \leq 0.01$, $***P \leq 0.001$, $****P \leq 0.0001$ and 'ns' is non-significant.

RESULTS

Sequence and backbone-dependent effects of ASOs on TLR7/8 sensing

We initially investigated the activity of a panel of 11 2′OMe gapmer ASOs targeted to the mRNA of the innate immune sensor cGAS, on immune responses of undifferentiated THP-1 cells. Surprisingly, overnight pre-treatment with the ASOs led to strong potentiation of IP-10 and TNF-α production upon R848 stimulation of TLR7/8 in the cells, for select ASOs (e.g. ASO2, ASO9, ASO11, but not ASO4 – Figure 1A). Previous studies have reported that T-rich PS oligonucleotides could promote TLR8 sensing, while inhibiting TLR7 (24,25). Since THP-1 can respond to both TLR7 and TLR8 ligands (26), we speculated that the sequence-specific effect of the ASOs on R848 sensing seen here could be due to their different activities on TLR7 and TLR8. To define this, we next tested our panel of sequences in HEK 293 cells stably expressing TLR7 or TLR8 (referred

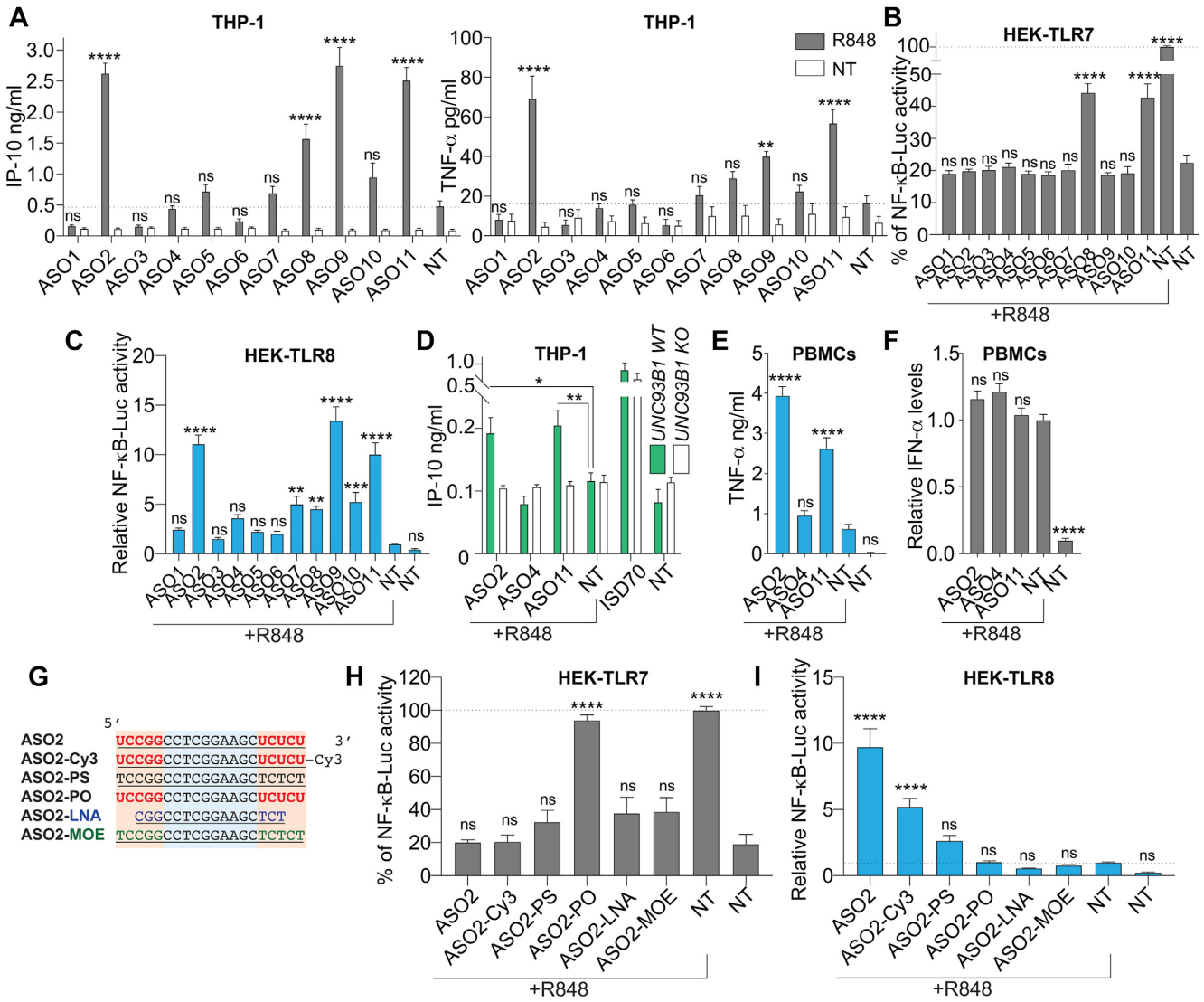

Figure 1. ASO-dependent modulation of R848 sensing by TLR7/8. (**A**) Wild-type THP-1 pre-treated overnight with 100 nM indicated ASO targeted to cGAS (Supplementary Table S1), were stimulated or not (non-treated [NT]) with 1 μg/ml R848 for 8.5 h, and IP-10 (left panel) and TNF-α (right panel) levels in supernatants determined by ELISA. Data shown are averaged from three (left) or two (right) independent experiments in biological triplicate (± s.e.m. and ordinary one-way ANOVA with Dunnett's multiple comparison tests to the 'R848 without ASO' condition are shown). There was no basal effect of the ASOs on NT cells for either cytokines. (B, C) HEK-TLR7 (**B**) and HEK-TLR8 (**C**) cells expressing an NF-κB-luciferase reporter were treated with 500 nM indicated ASOs for 50 min prior to stimulation with 1 μg/ml R848. NF-κB-luciferase levels were measured after overnight incubation. Percentages (B) or fold increases (C) relative to the condition 'R848 without ASO' condition are averaged from three independent experiments in biological triplicate (± s.e.m. and ordinary one-way ANOVA with Dunnett's multiple comparison tests to the NT condition [B] or the 'R848 without ASO' condition [C] are shown). (**D**) *UNC93B1*-deficient THP-1 (KO) and matched controls with rescued *UNC93B1* expression (WT) were treated with 100 nM ASO overnight, prior to stimulation with 1 μg/ml R848 for 24 h and IP-10 levels in supernatants determined by ELISA. Data shown are averaged from two independent experiments in biological triplicate for each cell line (± s.e.m and unpaired *t*-tests are shown). The cGAS ligand ISD70 was used at 2.5 μg/ml as positive control to induce IP-10. (E, F) PBMCs from two blood donors were incubated 20–45 min with 100 nM ASO, and stimulated with 0.5 μg/ml R848 for 4 h prior to TNF-α ELISA (**E**), or 24 h prior to IFN-α ELISA (**F**). (E) Data shown are averaged from two blood donors in biological triplicate (± s.e.m. and ordinary one-way ANOVA with Dunnett's multiple comparison tests to the 'R848 without ASO' condition are shown). (F) Data were normalised to the condition 'R848 without ASO' to limit variations between patients, and are averaged from 2 blood donors in biological triplicate (± s.e.m. and Brown-Forsythe and Welch ANOVA with Dunnett's T3 multiple comparison tests to the 'R848 without ASO' condition are shown). (**G**) [cGAS]ASO2 sequence variants used. The central DNA region is highlighted in blue. For the 3′ and 5′ flanking regions (highlighted in orange), the DNA bases are in black, the 2′OMe bases in red, the LNA bases in blue and the 2′MOE bases in green. Underlined bases are on a PS backbone. (H, I) HEK-TLR7 (**H**) and HEK-TLR8 (**I**) cells expressing an NF-κB-luciferase reporter were treated with 500 nM indicated ASOs for 20 min prior to stimulation with 1 μg/ml R848. NF-κB-luciferase levels were measured after overnight incubation. Percentages (H) or fold increases (I) relative to the condition 'R848 without ASO' condition are averaged from three (**I**) or two (**H**) independent experiments in biological triplicate (± s.e.m and ordinary one-way ANOVA with Dunnett's multiple comparison tests to the NT condition [H] or the 'R848 without ASO' condition [I] are shown). * $P \leq 0.05$, ** $P \leq 0.01$, *** $P \leq 0.001$, **** $P \leq 0.0001$, ns: non-significant.

to as HEK-TLR7 and HEK-TLR8 hereafter), along with an NF-κB-luciferase reporter (Figure 1B, C and Supplementary Figure S1A, B). Interestingly, we found that most ASOs strongly inhibited TLR7 sensing of R848, with the exception of ASO8 and ASO11, which were less potent inhibitors (Figure 1B). Conversely, and directly aligning with our observations in THP-1 cells, several ASOs strongly potentiated TLR8 sensing of R848 (e.g. ASO2, ASO9 and ASO11 – Figure 1C). The ASOs on their own did not stimulate TLR7 or TLR8 (Supplementary Figure S1A, B). Focusing on ASO2 and ASO11, which equally potentiated TLR8 but had different activities on TLR7, we validated further their TLR7/8-dependent activity in THP-1 lacking *UNC93B1,* which is essential to TLR7/8 signalling (20). The potentiation effect of ASO2 and ASO11 on R848 sensing was not seen in THP-1 lacking *UNC93B1*, but could be restored upon reconstitution of *UNC93B1-Citrine* expression (20) (Figure 1D), thereby supporting the involvement of TLR7/8 in this effect. In addition, stimulation of human peripheral blood mononuclear cells (PBMCs) with ASO2 and ASO11 strongly potentiated R848 induced TNF-α, but did not impact IFN-α levels, indicative of a preferential effect on TLR8 sensing of R848 (26) (Figure 1E, F). This effect on IFN-α and TNF-α was not related to TLR9 activation of PBMCs by the ASOs, since ASO2 did not activate TLR9 signalling in HEK-TLR9 cells, while ASO11 did (Supplementary Figure S1C). To define whether this effect of the ASOs on TLR7/8 was dependent on their backbone or base modifications, we next studied a series of ASO variants based on the sequence of ASO2 (Figure 1G–I). Analyses of these variants in HEK-TLR7 cells stimulated with R848 revealed that all ASO2 variants containing a PS backbone inhibited TLR7, independent of the type of base modifications used (DNA only, 2′OMe, LNA or 2′MOE) (Figure 1G, H, Supplementary Table S1). Conversely, potentiation of R848 sensing by TLR8 was directly dependent on the 5′ and 3′ end base modifications, with 2′OMe giving the best potentiation in this sequence context (Figure 1G, I). Addition of a 3′ end Cy3 linker decreased this potentiation of TLR8 sensing, while substitution of 2′OMe bases with 2′MOE or LNA bases ablated the potentiation. The PS backbone was necessary for TLR8 potentiation; it was not, however, sufficient for this effect by itself, since the 2′OME and LNA ASO2 variants were also synthesised on a PS backbone, and only limited potentiation was seen with the variant featuring the PS modification only (ASO2-PS). Collectively these results demonstrated that PS ASOs could display potent TLR7/8 immunomodulation, in a sequence-dependent manner.

Screen to identify ASOs with low TLR7 inhibition and high TLR8 potentiation

Our observation of TLR7 inhibition and TLR8 potentiation by select PS ASOs aligned with the previous reports that T-rich PS oligonucleotides could promote similar activities (24,25). However, our finding that some 2′OMe ASO sequences had less inhibitory activity on TLR7 (e.g. ASO8 and ASO11) suggested that TLR7 inhibition promoted by the PS backbone may be counterbalanced in select 2′OMe gapmer ASOs. We reasoned that defining the modalities of this activity could help design ASOs with reduced immunosuppressive activities towards TLR7. In addition, the observation that ASO11 was able to potentiate TLR8 sensing of R848 while preserving TLR7 activity, suggested that the activities on TLR7 and 8 were not governed by the same sequence determinants.

To characterize these observations further, we screened a library of 192 2′OMe ASOs. It is noteworthy that these ASOs were designed to target 4 different transcripts (48 ASOs each), with a minimum of single base increments between the ASOs (Supplementary Table S2). The screen was performed at two different ASO concentrations for each TLR and measured their impact on NF-κB-luciferase induction by R848 in HEK-TLR7 and HEK-TLR8 cells (Figure 2A, B and Supplementary Table S2). In agreement with the initial panel ASOs, we found that the majority of ASOs used at 500 nM strongly suppressed TLR7 sensing. As such, 78% of the ASOs reduced R848 activity on TLR7 by >80%, and only two ASOs reduced TLR7 sensing by less than 40% at both concentrations (Figure 2A and Supplementary Table S2 – ASOs '[CDKN2B-AS1]-852' and '[LINC-PINT]-2504', referred to as ASO852 and ASO2504 hereafter). Conversely, the effect of ASOs on TLR8 potentiation was diverse across ASOs with 51% of the ASOs potentiating R848 sensing by at least 2-fold at 100 nM (Figure 2B).

Importantly, while both displaying low TLR7 inhibition, ASO852 and ASO2504 had distinct activities on TLR8 (Figure 2A, B and Supplementary Table S2). ASO dose-response studies in HEK-TLR7 and HEK-TLR8 cells confirmed that ASO2504 and ASO852 had little impact on R848 sensing by TLR7 compared to ASO4, however ASO852 potentiated TLR8 sensing significantly more than ASO4 (Figure 2C). Analyses of the impact of ASO852 on various doses of R848 revealed that it decreased the sensitivity of TLR7 to R848 by ∼2.5-fold (Figure 2D). However, ASO852 treatment increased the activity of R848 on TLR8 ∼13-fold (Figure 2D).

TLR7 inhibition by 2′OMe ASOs can be reverted by CUU terminal motifs

MEME motif discovery analysis (27) of 19 ASOs with lowest TLR7 inhibitory activity based on the above screens led to the observation that the 2′OMe regions of the ASOs exhibiting terminal 5′ and 3′ 'C' bases were over-represented in 8 sequences, along with uridine residues (Figure 3A, Supplementary Table S2). In addition, analysis of a family of sequences from the screen (referred to as the PINT family) with single base increments suggested different inhibitory activity on TLR7 for closely related sequences (Figure 3B, C and Supplementary Table S2—from ASO '[LINC-PINT]-108' to [LINC-PINT]-116', referred to as ASO108-ASO116). Validation of the PINT family of ASOs in HEK-TLR7 cells confirmed that ASO111 only was capable of blocking TLR7 activation by R848 in this family (Figure 3B, C). Critically, sequence alignment analyses revealed that ASO111 was the only sequence lacking a CUU/CUT/CTT motif in its 5′ or 3′ end regions (Figure 3C). Since [cGAS]ASO11 also harboured such terminal 2′OMe CUU motifs in both its 5′ and 3′-ends (along with 4 other sequences harbouring the enriched motif in Figure

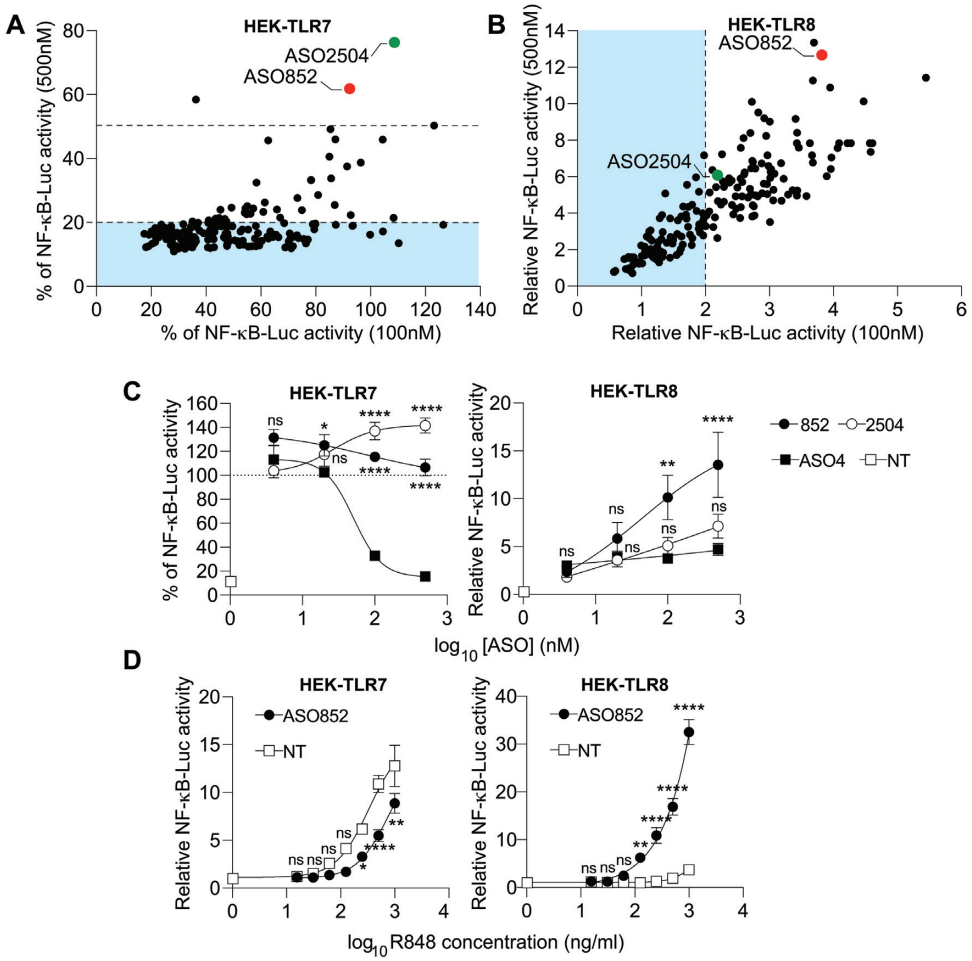

Figure 2. Identification of ASOs with low TLR7 inhibition and high TLR8 potentiation. (A, B) HEK-TLR7 (**A**) and HEK-TLR8 (**B**) cells expressing an NF-κB-luciferase reporter were treated with 100 nM or 500 nM indicated ASOs for 20–50 min prior to stimulation with 1 μg/ml R848. NF-κB-luciferase levels were measured after overnight incubation. Percentages (A) or fold increases (B) relative to the condition 'R848 without ASO' are averaged from biological duplicates (averaged data are provided in Supplementary Table S2). Stimulations with 100 nM and 500 nM ASO were performed in independent experiments (data shown for each concentration is from a single experiment). [CDKN2B-AS1]-852, and [LINC-PINT]-2504 are referred to as ASO852 and ASO2504, and are highlighted on the plot. ASOs with ≥80% reduction of TLR7 activity at 500 nM (A) and ≤2-fold TLR8 potentiation at 100 nM (B) are highlighted with blue shading. (C, D) HEK-TLR7 (left panels) and HEK-TLR8 (right panels) cells expressing an NF-κB-luciferase reporter were treated with increasing ASOs concentrations (4, 20, 100 and 500 nM) (**C**) or with 500 nM ASOs (**D**) for 20 min prior to stimulation with 1 μg/ml R848 (C) or with increasing R848 concentrations (0.0156, 0.031, 0.062 0.125, 0.250, 0.5, 1 μg/ml) (D). NF-κB-luciferase levels were measured after overnight incubation. Percentages (left panels) or fold increases (right panels) relative to the condition 'R848 without ASO' (C) or NT condition (D) are averaged from two independent experiments in biological triplicate (± s.e.m and ordinary two-way ANOVA with Dunnett's multiple comparison tests to the ASO4 condition [C] or R848 only condition [D] are shown). * $P \leq 0.05$, ** $P \leq 0.01$, *** $P \leq 0.001$, **** $P \leq 0.0001$, ns: non-significant.

3A), we next tested [cGAS]ASO11 variants (ASO11-Mut1 and ASO11-Mut2) in which the 5′ and 3′ end 2′OMe regions were swapped with these of ASO2, which lacked such 'CUU' motifs and was a potent repressor of TLR7 (Figure 3D, E). Aligning with a key role for both the 5′ and 3′ end regions, both ASO11 mutants significantly increased TLR7 inhibition compared to the parental ASO11 (Figure 3D, E). These findings collectively indicated that 5′ and 3′ CUU motifs were important modulators of TLR7 inhibition by the 2′OMe-PS ASOs.

TLR8 potentiation is driven by the central DNA region and the 5′-end of 2′OMe PS ASOs

We also analysed the PINT family (ASO108–116) and [cGAS]ASO11 mutants for TLR8 potentiation. While two sequences were more potent (e.g. ASO108 and ASO110), most of the sequences displayed similar TLR8 potentiation, suggesting that the central region of these molecules was predominantly involved in TLR8 modulation (Figure 3C, F). Similarly, the ASO11 mutations only mildly impacted TLR8 potentiation, although addition of the ASO2 3′ end (ASO11-Mut1) significantly decreased, while the ASO2 5′ end (ASO11-Mut2) significantly increased TLR8 sensing (Figure 3D, G). These results indicated that the control of TLR8 potentiation by 2′OMe-PS ASO was predominantly governed by the central 10-mer DNA region of the ASO, but that the 2′OMe ends also played a role.

In further support of a contribution by the 5′-end region of the ASOs, we noticed that most of the top 20 potentiators of TLR8 sensing in our screen had a terminal 5′-U (14 out of 20), while occurrence of such terminal 5′-U was much

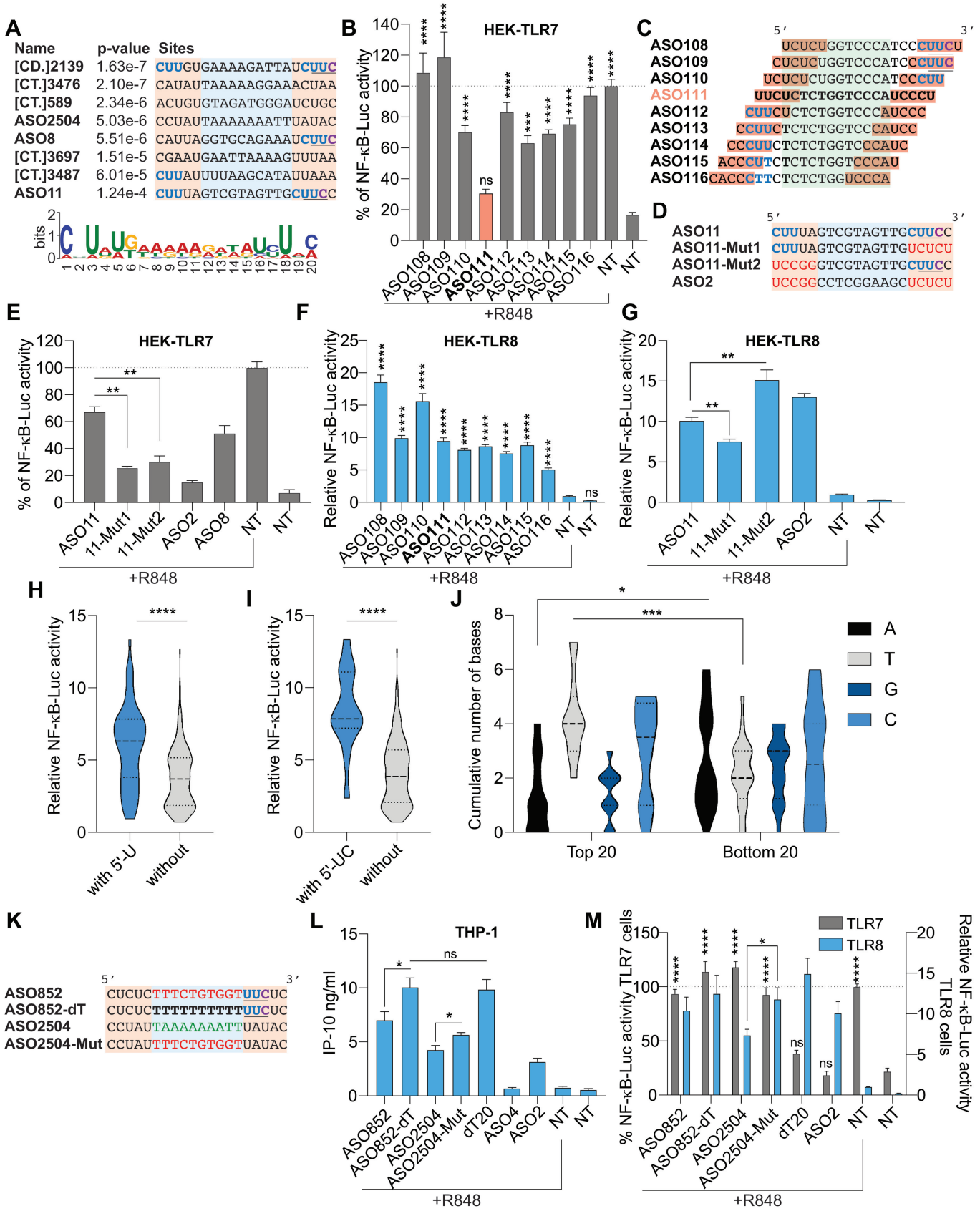

Figure 3. Identification of molecular determinants of ASO effect on TLR7/8. (**A**) Top: sequence alignments of ASOs from the screens on HEK-TLR7 cells (Figure 2A) which displayed low TLR7 inhibition at 100 nM and harboured significantly enriched motif (see Supplementary Table S2 for detail of the

less frequent among the bottom 20 potentiators (3 out of 20) (Supplementary Table S2). Comparing sequences of the 192 ASOs with or without terminal 5′-U confirmed a significantly increased potentiation of TLR8 sensing by sequences harbouring a terminal 5′-U (Figure 3H and Supplementary Table S2). A similar trend was observed for terminal 5′-UC motifs (present in 9/20 of the top ASOs - Figure 3I and Supplementary Table S2). Critically, ASO108 and ASO110 were the only two ASOs from the PINT family to harbour such terminal 5′-UC motifs, which were also present in ASO2 and ASO11-Mut2.

We also noted that the central 10-mer DNA region of the TLR8 potentiating ASO852 contained a central T-rich region (TTTCTGTGGT), while that of ASO2504 was A-rich (TAAAAAAATT). Comparison of the central DNA regions of the top and bottom 20 potentiators of TLR8 sensing confirmed a significantly increased proportion of thymidine residues in the ASOs potentiating TLR8 sensing the most—with a median of 4 central thymidines (Figure 3J and Supplementary Table S2). Since this observation was directly aligned with previous reports that T-rich regions were important for TLR8 potentiation (24,25), we mutated ASO852 to ASO852-dT, containing a central stretch of 10 dTs (Figure 3K). In addition, we swapped the central 10-mer DNA region of ASO2504 with that of ASO852 to result in ASO2504-Mut (Figure 3K), since ASO2504 did not potentiate TLR8 as much as ASO852. Comparison of the activities of these oligonucleotides on R848 sensing was performed in THP-1 cells, HEK-TLR7 and HEK-TLR8 cells (Figure 3L, M and Supplementary Figure S1A, B, D). The 2504-Mut ASO was significantly more potent in driving IP-10 production in THP-1 cells and NF-κB luciferase in HEK-TLR8 cells, an observation in support of a critical role for the central T-rich 10-mer DNA region of the ASOs in their effects on TLR8. In addition, ASO852-dT was also more potent at inducing IP-10 than ASO852, reaching similar levels of stimulation to those obtained with a 20-mer dT PS oligonucleotide (dT20) in THP-1 cells. Conversely, substitutions of the central regions for ASO852-dT and ASO2504-Mut did not significantly impact TLR7 sensing of R848, while dT20 blocked TLR7 activation. None of these ASOs used alone in HEK-TLR7, HEK-TLR8 or THP-1 cells impacted NF-κB luciferase activity in HEK cells and IP-10 production in THP-1 (Supplementary Figure S1A, B, D). However, increasing the central T-rich region of ASO852 further potentiated its basal activity on TLR9-driven NF-κB luciferase—aligning with the observation that dT20 alone also acted as a mild TLR9 ligand in HEK-TLR9 cells (Supplementary Figure S1C).

TLR8 potentiation of R848 by ASOs leads to IRF activation

The capacity of ASO852-dT to strongly potentiate IP-10 production upon R848 sensing was confirmed in two other TLR8 expressing AML cell lines (MOLM13 and OCI-AML3; Figure 4A), and was readily observable with as little as 4 to 20 nM ASO852-dT (Figure 4B). Given the high production of IP-10 seen, suggestive of IRF activation, we tested the activity of the ASO852-dT series in HEK-TLR8 cells expressing CCL5-Luciferase or IFN-β-Luciferase reporters, which are driven by IRFs (28,29). While R848 alone did not activate either reporters, co-stimulation with the oligonucleotides potentiated both promoters, with ASO852-dT and dT20 being the most potent, followed by ASO852/2504-Mut, and ASO2504 being the least potent (Figure 4C); this finding thus mirrors the results obtained with IP-10 production in THP-1 cells (Figure 3L). To further support induction of an IRF-driven response, we carried out RT-qPCR analyses of several IRF-driven genes including *IFNB1*, at 4 h after R848 stimulation of THP-1 cells. While little induction of *IFIT1*, *RSAD2*, *IFI44* and *IFNB1* was seen with R848 only, all these genes were significantly increased by co-stimulation with ASO852-dT (Figure 4D). We had observed that ASO co-stimulation strongly increased the sensitivity of TLR8 to R848 in HEK-TLR8 cells (Figure 2D), suggesting that the effect seen on *IFNB1*

←

17 ASOs used in this analysis). [CD.] is CDKN2B-AS1; [CT.] is CTNNB1. The central DNA region is highlighted in blue and the 3′ and 5′ 2′OMe flanking regions are highlighted in orange. Bottom: MEME pictogram of the relative frequency of bases constituting the non-inhibitory motif. CUU motifs are in bold blue, while UUC motifs are underlined. (B, E) HEK-TLR7 cells expressing an NF-κB-luciferase reporter were treated with 100 nM (**B**) or 500 nM (**E**) indicated ASOs for 20 min prior to stimulation with 1 μg/ml R848. NF-κB-luciferase levels were measured after overnight incubation. Percentages relative to the condition 'R848 without ASO' are averaged from three (**B**) or two (E) independent experiments in biological triplicate (± s.e.m and ordinary one-way ANOVA with Dunnett's multiple comparison tests to the NT condition [B] or Mann-Whitney U tests [E] are shown). (**C**, **D**) Sequence alignments of ASOs from the PINT series (**C**) and [cGAS]ASO11 variants (**D**). (C) The conserved region between all the sequences is highlighted in green. The 2′OMe flanking regions are highlighted in orange. (D) The central DNA region is highlighted in blue and the 3′ and 5′ 2′OMe flanking regions are highlighted in orange. (**C**, **D**) CUU motifs are in bold blue, while UUC motifs are underlined. (F, G) HEK-TLR8 cells expressing an NF-κB-luciferase reporter were treated with 100 nM (**F**) or 500 nM (**G**) indicated ASOs for 20 min prior to stimulation with 1 μg/ml R848. NF-κB-luciferase levels were measured after overnight incubation. Fold increases relative to the condition 'R848 without ASO' are averaged from three (F) or two (G) independent experiments in biological triplicate (± s.e.m and ordinary one-way ANOVA with Dunnett's multiple comparison tests to the NT condition [F] or Mann–Whitney *U* tests [G] are shown). (H, I) 192 ASOs from the screen sorted into two groups according to presence/absence of terminal 5′mU (**H**) or 5′mUmC (**I**), and fold increase of NF-κB-luciferase levels to R848 only (using 500 nM ASOs – Supplementary Table S2) are shown as violin plots for each population. Mann–Whitney *U* tests are shown. (**J**) The central 10 DNA bases of the top and bottom 20 TLR8 potentiators from the 192 ASOs screened (see Supplementary Table S2) was analysed for base content. The violin plots show the distribution of the cumulative number of each central base for both ASO populations. Ordinary two-way ANOVA with Sidak's multiple comparison tests are shown. (**K**) ASO852 and ASO2504 variants. The central DNA region is highlighted in blue and the 3′ and 5′ 2′OMe flanking regions are highlighted in orange. (**L**) WT THP-1 were pre-treated overnight with 100 nM ASO, and stimulated with 1 μg/ml R848 for 7 h and IP-10 levels in supernatants determined by ELISA. Data shown are averaged from two independent experiments in biological triplicate (± s.e.m. and unpaired *t*-tests are shown). (**M**) HEK-TLR7 and HEK-TLR8 cells expressing an NF-κB-luciferase reporter were treated with 500 nM indicated ASOs for 20 min prior to stimulation with 1 μg/ml R848. NF-κB-luciferase levels were measured after overnight incubation. Percentages or fold increases relative to the condition 'R848 without ASO' condition are averaged from three independent experiments in biological triplicate (± s.e.m and ordinary one-way ANOVA with Dunnett's multiple comparison tests to the NT condition [TLR7] or Mann-Whitney U test [TLR8] are shown). * $P \leq 0.05$, ** $P \leq 0.01$, *** $P \leq 0.001$, **** $P \leq 0.0001$, ns: non-significant.

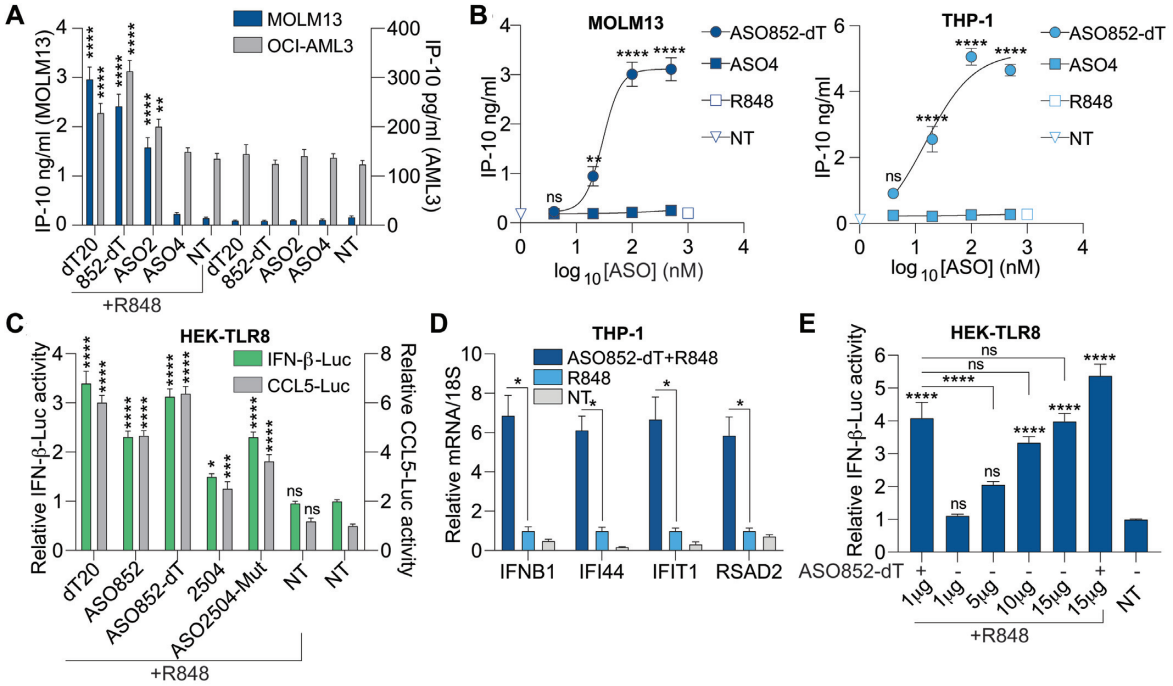

Figure 4. Characterization of ASOs potentiation of R848 sensing by TLR8. (**A**) MOLM13 and OCI-AML3 cells were incubated overnight with 500 nM ASOs, stimulated with 1 μg/ml R848 for 8 h (MOLM13) or 24 h (OCI-AML3), and IP-10 levels in supernatants determined by ELISA. Data shown are averaged from five (MOML13) or four (OCI-AML3) independent experiments for all conditions with exception of the ASO only conditions (carried out in two independent experiments) in biological triplicate (± s.e.m. and ordinary one-way ANOVA with Dunnett's multiple comparison tests to the 'R848 without ASO' condition are shown). (**B**) MOLM13 and THP-1 were incubated overnight with increasing doses of ASOs (4, 20, 100, 500 nM), stimulated with 1 μg/ml R848 for 8 h and IP-10 levels in supernatants determined by ELISA. Data shown are averaged from two independent experiments in biological triplicate (± s.e.m. and ordinary two-way ANOVA with Dunnett's multiple comparison tests to the ASO4 condition are shown). (**C**) HEK-TLR8 cells expressing a CCL5-luciferase reporter or an IFN-β-luciferase reporter were treated with 500 nM indicated ASOs for 20 min prior to stimulation with 1 μg/ml R848. Luciferase levels were measured after overnight incubation. Data are shown as fold increase to NT condition, and are averaged from two independent experiments in biological triplicate (± s.e.m. and ordinary one-way ANOVA with Dunnett's multiple comparison tests to the NT condition are shown). (**D**) WT THP-1 were incubated overnight with 500 nM ASO852-dT (or NT), and stimulated or not for 4 h with 1 μg/ml R848, prior to RNA purification. Expression of panel of four IRF-driven genes was analysed by RT-qPCR. Expression of the indicated genes was reported to *18S* expression, and further normalised to the average of the 'R848 without ASO' condition. Data shown represent the average of two independent experiments conducted in biological duplicate (± s.e.m. and Mann–Whitney *U* tests are shown). (**E**) HEK-TLR8 cells expressing an IFN-β-luciferase reporter were treated with 500 nM ASO852-dT (or NT) for 20 min prior to stimulation with increasing doses of R848 (1, 5, 10, 15 μg/ml). IFN-β-luciferase levels were measured after overnight incubation. Data are shown as fold increase to NT condition, and are averaged from two independent experiments in biological triplicate (± s.e.m. and ordinary one-way ANOVA with Tukey's multiple comparison tests to the NT condition and selected pairs of conditions are shown). * $P \leq 0.05$, ** $P \leq 0.01$, *** $P \leq 0.001$, **** $P \leq 0.0001$, ns: non-significant.

induction may be due to increased sensitivity of TLR8 to R848. IFN-β-Luciferase reporter dose-responses to R848 (ranging from 1 to 15 μg/ml) in HEK-TLR8 cells demonstrated that high doses of R848 engaged the IFN-β response in these cells to a similar extent as with low dose R848 + ASO852-dT (Figure 4E). Collectively, these results suggest that ASOs such as ASO852-dT facilitate activation of IRF-driven responses otherwise only achievable with very high doses of R848.

Identification of gene-targeting ASOs potentiating TLR8 sensing

We next sought to establish proof-of-principle that bi-functional ASOs combining gene-targeting and TLR8 potentiation (while avoiding TLR7 inhibition) could be achieved. For this purpose, we tested a panel of 48 2′OMe ASOs designed against the mRNA of the human *HPRT* gene. Preliminary studies in HeLa cells suggested that 29 out of the 48 ASOs significantly reduced *HPRT* mRNA levels by at least 50% at 10 nM (Supplementary Figure S2 and Table S3). We therefore focused on this sub-panel of 29 sequences for the following experiments comparing gene-targeting, TLR7 inhibition and TLR8 potentiation of R848 sensing (Figure 5A–C, respectively). In agreement with our previous findings, these experiments confirmed that most ASOs blocked TLR7 activation by R848, with the notable exceptions of [HPRT]ASO551, ASO660-663 and ASO665 ASOs (Figure 5B). Critically, each of these sequences harboured at least one CUU/CUT motif in their 5′ or 3′ end, further suggesting an important role for these motifs in the retention of TLR7 sensing (Figure 5D). Interestingly, both ASO551 and ASO662 ASOs harboured one 5′-CUU and one 3′-UUC motif, but ASO551 ASO was the only ASO entirely preserving TLR7 sensing. Since the position of these 5′-CUU and 3′-UUC motifs varied between both ASOs, optimal positioning of the CUU motif may be in the terminal 5′-end of the ASOs, indicating that terminal 3′-end UUC motifs may also be important. At this point, we note again that [LINC-PINT]ASO109 and [cGAS]ASO8 also had such

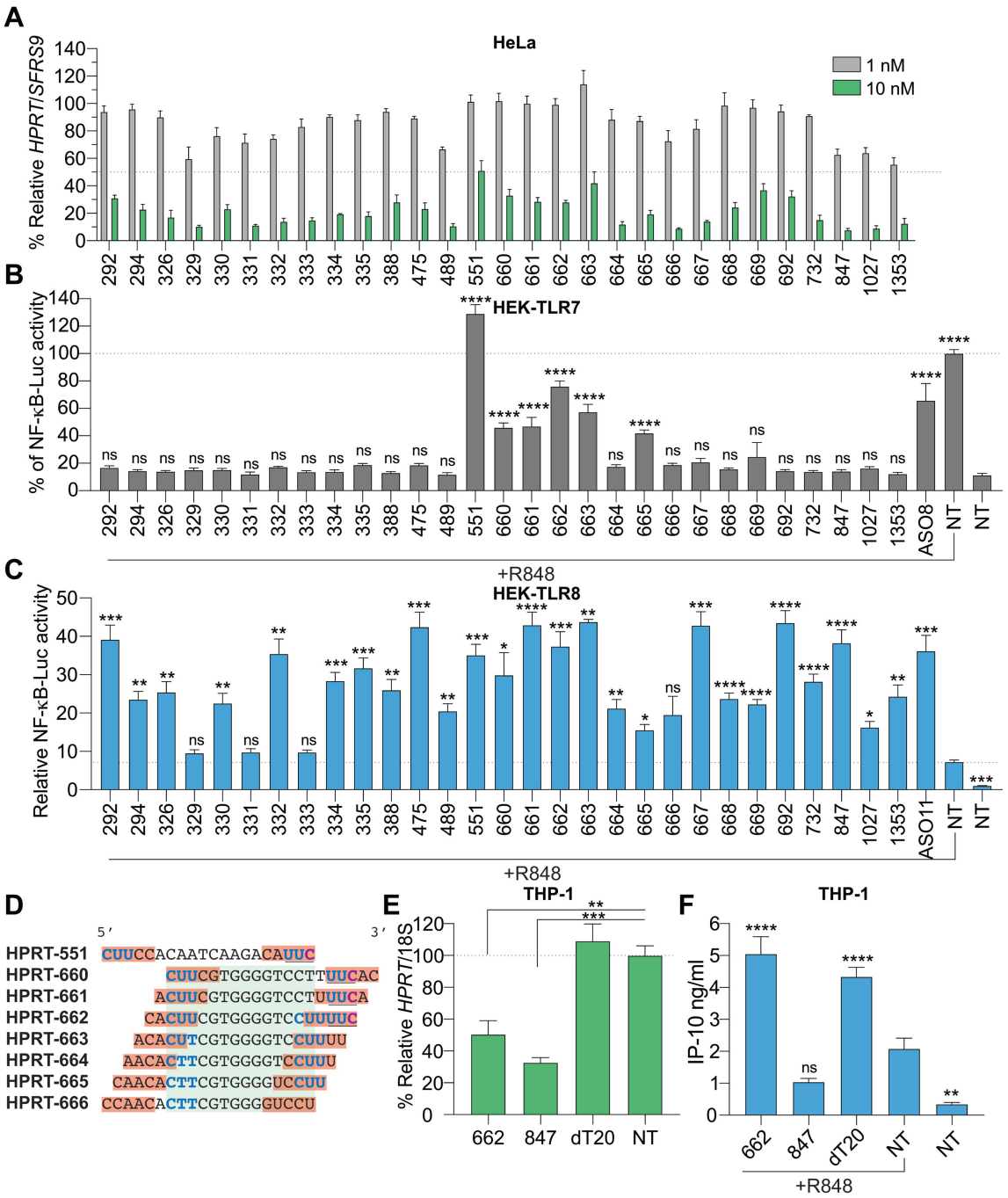

Figure 5. Rational selection of *HPRT*-targeting ASOs exhibiting TLR8 potentiation. (**A**) HeLa cells were reverse-transfected with indicated *HPRT*-targeting ASO quantities as detailed in the Materials and Methods section and Supplementary Table S3, and *HPRT* levels measured by RT-qPCR after 24h incubation. *HPRT* levels were reported to *SFRS9* expression, and further normalised to the average of the non-targeting ASONC1 and ASONC5 control conditions. Data shown represent the average of three independent experiments conducted in biological triplicate (± s.e.m). (B, C) HEK-TLR7 (**B**) and HEK-TLR8 (**C**) cells expressing an NF-κB-luciferase reporter were treated with 500 nM ASOs for 20 min prior to stimulation with 1 μg/ml R848. NF-κB-luciferase levels were measured after overnight incubation. Percentages (B) or fold increases (C) relative to the condition 'R848 without ASO' (B) or NT condition (C) are averaged from three independent experiments in biological triplicate (± s.e.m and ordinary one-way ANOVA with Dunnett's multiple comparison tests to the NT condition [B] or the 'R848 without ASO' condition [C] are shown). (**D**) Selected HPRT ASO sequences with low TLR7 inhibition. The conserved region between all the sequences is highlighted in green. The 2′OMe flanking regions are highlighted in orange. CUU motifs are in bold blue, while UUC motifs are underlined. (E, F) WT THP-1 were incubated overnight with 100 nM ASOs. The next day, the cells were treated with lipofectamine 2000 (at 2.5 μl/ml, to enhance cytoplasmic delivery of the ASOs), just before R848 stimulation (1 μg/ml for F only). Supernatants were collected after 8 h for IP-10 ELISA (**F**), and cells lysed for RNA purification after 24 h (**E**). (E) *HPRT* levels were reported to *18S,* and normalised to NT condition. Data are averaged from four (E) or three (F) independent experiments in duplicate (± s.e.m. and ordinary one-way ANOVA with Dunnett's multiple comparison tests to the 'R848 without ASO' condition [F] or Mann–Whitney *U* tests [E] are shown). * $P \leq 0.05$, ** $P \leq 0.01$, *** $P \leq 0.001$, **** $P \leq 0.0001$, ns: non-significant.

terminal 3′-UUC motifs. These data align with the MEME motif that showed terminal 5′ and 3′ Cs were prevalent in non-inhibitory sequences (Figure 3A).

In addition, most ASOs significantly potentiated TLR8 sensing to varying degrees, with the exception of 4 HPRT ASOs (ASO329, ASO331, ASO333, ASO666) (Figure 5C). Based on these analyses, we selected ASO662 as an ASO with good *HPRT* targeting (>70% at 10 nM), retaining TLR7 activity (∼80%), and potentiating TLR8 sensing of R848 ∼5-fold. In addition, we selected ASO847 as an ASO with high gene targeting activity (>93%), strong TLR7 inhibition and TLR8 potentiating activity close to that of ASO662. The two ASOs were transfected in THP-1 cells and led to significant *HPRT* down-regulation, which was more pronounced for ASO847 - aligning with the data from HeLa cells (Figure 5A and E). In addition, following the same transfection protocol, ASO662 strongly potentiated IP-10 production induced by R848 (to a similar level as with the control dT20 oligonucleotide) (Figure 5F). Unexpectedly, ASO847 failed to increase IP-10 production following R848 co-stimulation, which may be attributed to its inhibitory effect on TLR7, which is also functional in THP-1 cells (26).

DISCUSSION

Imiquimod, a small molecule-agonist of TLR7, has been approved for more than two decades to treat basal cell carcinoma, acting through the production of type-I IFN and recruitment of CD8+ T cells to the tumors (30). Several other TLR7 or TLR7/8 agonists have shown promise in preclinical cancer immunotherapy trials, including Resiquimod, Gardiquimod, or 852A (31). However, while TLR7 agonists principally induce type-I IFN through plasmacytoid dendritic cells (pDCs) activation in humans, dual TLR7/8 agonists, due to their activity on TLR8, also activate potent TNF-α and IFN-γ production from monocytes and NK cells, which are important anti-tumoral effectors (32,33). TLR7/8 dual agonists such as R848 or 3M-052 may therefore offer additional anti-tumoral activities compared to TLR7 single agonists, although little is known of the therapeutic potential of TLR8 activation since it is not functional in mice (34). Nonetheless, systemic delivery of TLR7 and TLR7/8 agonists has been associated with toxicities including 'flu-like' symptoms in patients when threshold doses are exceeded (35,36), indicating that their therapeutic application is directly constrained by dosing.

In the current study, we revisited findings made more than 10 years ago, namely that PS-oligonucleotides containing DNA bases can synergise with R848 to activate TLR8 while abolishing signaling through TLR7 (24,25). In contrast to these studies, however, we demonstrated that select 2′OMe gapmer oligonucleotides on a PS backbone could potentiate TLR8 sensing while preserving TLR7 activation. Our analyses indicate that the 2′OMe gapmer oligonucleotide combination can increase the sensitivity of TLR8 to R848 >10 fold. As such, when combined with ASO852-dT, 1 μg/ml of R848 activated IFN-β responses otherwise requiring 10–15 μg/ml of R848, and less than 0.1 μg/ml R848 led to as much NF-κB reporter induction as 1 μg/ml did without the gapmer oligonucleotides. Potentiation was not limited to the dual TLR7/8 agonist R848 and was also seen with CL075 (TLR8 agonist), Loxoribine (TLR7 agonist), and marginally with Gardiquimod (TLR7 agonist) (Supplementary Figure S3), in accord with previous reports (24,25). These results collectively suggest that strategies relying on targeted delivery of PS-oligonucleotides such as ASO852-dT may help alleviate the dose-limiting toxicities of systemic TLR7 and 7/8 agonists, for instance by decoupling the delivery of the oligonucleotides from that of the TLR7 and 7/8 agonists. Whether this strategy could be therapeutically effective in a real-world setting is however not known and will require further studies.

Mechanistically, based on current models, potentiation of the 2′OMe gapmer ASOs can be attributed to the binding of R848 to the first site of TLR8, while the oligonucleotides or their degradation products bind a second site of the TLR8 horseshoe structure (37). Although we have not directly studied the potentiation of RNA molecules (including by unmodified siRNAs and microRNA mimics) by 2′OMe ASOs, we speculate that such potentiation is also possible since uridine residues from degraded RNAs should structurally be interchangeable with R848 and bind the second site of TLR8 (37). Strikingly, modulation of R848 sensing by TLR7/8 did not require any transfection of the 2′OMe gapmer ASOs, and was presumably due to endocytosis by cell-surface receptors through the PS-DNA moiety (38), broadly supporting entry in the different cell types tested here (embryonic kidney cells [HEK 293 cells], monocytic cells [THP-1, MOLM13, OCI-AML3], primary macrophages and PBMCs). Since TLR7 inhibition of R848 was observed for many sequences lacking the capacity to potentiate TLR8 in HEK 293 cells, we can rule out that the differences seen in TLR8 potentiation were due to differential uptake efficacy of the 2′OMe gapmer ASOs. A similar reasoning can be applied for TLR7 inhibition, considering ASOs that potentiated TLR8 and had varying impact on TLR7 sensing (e.g. [cGAS]ASO2 and [cGAS]ASO11).

TLR8 potentiation by 2′OMe gapmer ASOs was predominantly influenced by their central DNA region, however the flanking 2′OMe regions were also at play as seen with [cGAS]ASO11 mutants, and the ASO2 PS oligonucleotide lacking 2′OMe flanks. Detailed sequence analyses from our screen data indicate that a terminal 5′-U/UC is also a positive factor for TLR8 potentiation, which is supported by ASO108 and ASO110 having greater activity than other sequences in that series with single base increments. In addition, potentiation was greater with a larger number of central dT (as directly evidenced with ASO852 and ASO852-dT, and ASO2504/2504-Mut), aligning with the reported preferential effect of Ts over other bases (24,25). In HEK-TLR8 cells, the PS backbone was necessary for TLR8 potentiation (aligning with other reports (24,25)) but not sufficient since ASO2 PS variants with LNA or 2′MOE flanking regions did not potentiate TLR8 sensing. This role of the PS backbone on TLR7 and TLR8 sensing may however relate to the increased stability of PS ASOs over PO ASOs, and their capacity to reach the endosomal compartment to modulate R848 detection. It is noteworthy that a PS-modified LNA/DNA ASO targeted to miR-16 was also capable of potentiating TLR8 sensing (39), indicating that select LNA gapmer or mixmer ASOs may also be

able to synergise with R848 and that the concept of PS-ASO potentiation of TLR8 is therefore not restricted to 2′OMe ASOs.

Albeit in a sequence-dependent manner, we found that >50% of the sequences tested in our screens could potentiate TLR8 sensing of R848 >2-fold. A similar observation was made for the ASOs designed to target *HPRT*. This underlines the high frequency of 2′OMe gapmer ASOs that are amenable to R848 co-stimulation (noting that a two-fold difference in R848 concentration was found to be critical for its associated toxicities *in vivo* (35)). While not always as consistent as other gapmer designs for knockdown efficacy, screening of inexpensive 2′OMe gapmer ASOs can be easily implemented to identify highly potent candidates. Here we provide proof-of-principle that rational selection of gene-targeting 2′OMe gapmer ASOs directed against *HPRT*, which can also synergise with dual TLR7/8 agonists, can easily be achieved. Such bifunctional molecules, combining gene targeting to immune stimulation, have already been described for siRNA scaffolds (40–42), or ASOs fused to TLR9 ligands (43), but have not previously been described for ASOs engaging with TLR7/8. With several on-going clinical trials assessing gene-targeting ASOs in cancer (e.g. danvatirsen and IONIS-AR-2.5$_{Rx}$), we propose that TLR8 recruitment by bifunctional ASOs and low-dose R848 may provide novel therapeutic avenues in cancer. In some instances, as seen with the case of ASO852-dT, some ASOs potentiating TLR8 sensing may also act as direct TLR9 ligands – thus increasing further their immunomodulatory effects in the context of cancer.

Beyond TLR8 potentiation, we demonstrate here that gapmer ASOs broadly suppress TLR7 sensing, and that this is a common feature of PS-modified ASOs, aligning with previous reports (24,25,44). Although select sequences may be more potent inhibitors than others (44), the inhibition of TLR7 by ASOs is clearly frequent, and poses the risk of unintended immune suppression against sensing of pathogenic TLR7 agonists. We have previously reported that TLR7/8 were significantly inhibited by fully modified 2′OMe oligonucleotides targeted to microRNAs, with select motifs strongly increasing inhibition (12), aligning with previous reports that 2′OMe bases acted as TLR7 antagonists (10). Unexpectedly, we found here that the gapmer design incorporating five 2′OMe bases on each flank of the 10-mer DNA region, could instead suppress the inhibitory effect on TLR7 sensing of PS-modified oligonucleotides.

Detailed analyses demonstrated the importance of CUU/CUT motifs in the 2′OMe regions of the gapmers, with sequences harbouring both terminal 5′-CUU and 3′-UUC being the least inhibitory of TLR7 (e.g. [HPRT]ASO551). While gapmer ASOs exhibiting such 5′ and 3′ motifs are relatively frequent and may be rationally selected at the design step, we note that additional end sequences are likely to also suppress TLR7 inhibition as seen with ASO2504 which did not harbour any CUU/UUC motif. Whether appending terminal 2′OMe 5′-CUU and 3′-UUC motifs to otherwise immunosuppressive ASOs could work to mitigate the global immunosuppressive effects seen on TLR7 remains to be defined, but our work demonstrates for the first time that PS-modified ASOs can be designed to evade TLR7 suppression. Importantly given the current development of asymmetric siRNAs with 2′OMe-containing PS regions (45), some of these observations may also be applicable to siRNA designs which would therefore benefit from design rules including terminal CUU/UUC 2′OMe motifs.

In conclusion, we provide the first proof-of-principle that gene targeting ASOs can be rationally selected to synergise with TLR7/8 engagement by small molecule agonists. We propose that the capacity of such ASOs to potentiate sensing of TLR8 could help resolve dose-toxicities previously reported for TLR7/8 dual agonists, and may open new therapeutic avenues to treat cancers with these ASOs. While the broad applicability of this bi-functional approach remains to be addressed with other gapmer chemistries, our work highlights the need for a better definition of the cross-over activities on immune responses by nucleic acid modifications currently used in oligonucleotide-based therapeutics. We demonstrate here that TLR7 is strongly suppressed by PS-oligonucleotides, and show that this can be mitigated by rational selection at the design step of 2′OMe gapmer ASOs. Independent studies indicate that TLR3, TLR9, AIM2 and cGAS sensing can also be inhibited by PS-oligonucleotides (15,16,44,46). Further studies are therefore needed to define the structural determinants of therapeutic PS-oligonucleotides governing these immune inhibitory effects, to avoid the risk of promoting intercurrent pathogenic infections in patients.

SUPPLEMENTARY DATA

Supplementary Data are available at NAR Online.

ACKNOWLEDGEMENTS

We thank E. Latz for the *UNC93B*-deficient and rescued THP-1 cells; L. Kats for the MOLM13 and OCI-AML3 cells; G. Scholz for pCCL5-Luc vector; K. Fitzgerald for pLuc-IFN-β; B.R.G. Williams for comments on the manuscript and R.E. Smith for helping with the preparation of the manuscript.

FUNDING

Australian National Health and Medical Research Council [1081167, 1124485 to M.P.G.]; Australian Research Council [140100594 Future Fellowship to M.P.G.]; Quebec Fonds de Recherche du Québec (FRSQ) – Santé [35071 to G.P.]; Fielding Foundation Fellowship [to C.N-P.]; Fielding Foundation Innovation Award [to M.P.G.]; Victorian Government's Operational Infrastructure Support Program. Funding for open access charge: Hudson Institute of Medical Research.

Conflict of interest statement. Mark A. Behlke and Kim A. Lennox are employed by Integrated DNA Technologies Inc. (IDT), a Danaher company, which offers oligonucleotides for sale similar to some of the compounds described in the manuscript. Mark A. Behlke owns equity in DHR, the parent company of IDT.

REFERENCES

1. Yin,W. and Rogge,M. (2019) Targeting RNA: A transformative therapeutic strategy. *Clin. Transl. Sci.*, **12**, 98–112.

2. Al Shaer,D., Al Musaimi,O., Albericio,F. and de la Torre,B.G. (2020) 2019 FDA TIDES (peptides and oligonucleotides) harvest. *Pharmaceuticals (Basel)*, **13**, 40.
3. Coutinho,M.F., Matos,L., Santos,J.I. and Alves,S. (2019) RNA therapeutics: how far have we gone? *Adv. Exp. Med. Biol.*, **1157**, 133–177.
4. Hornung,V., Guenthner-Biller,M., Bourquin,C., Ablasser,A., Schlee,M., Uematsu,S., Noronha,A., Manoharan,M., Akira,S., de Fougerolles,A. *et al.* (2005) Sequence-specific potent induction of IFN-alpha by short interfering RNA in plasmacytoid dendritic cells through TLR7. *Nat. Med.*, **11**, 263–270.
5. Kleinman,M.E., Yamada,K., Takeda,A., Chandrasekaran,V., Nozaki,M., Baffi,J.Z., Albuquerque,R.J., Yamasaki,S., Itaya,M., Pan,Y. *et al.* (2008) Sequence- and target-independent angiogenesis suppression by siRNA via TLR3. *Nature*, **452**, 591–597.
6. Krieg,A.M., Yi,A.K., Matson,S., Waldschmidt,T.J., Bishop,G.A., Teasdale,R., Koretzky,G.A. and Klinman,D.M. (1995) CpG motifs in bacterial DNA trigger direct B-cell activation. *Nature*, **374**, 546–549.
7. Pichlmair,A., Schulz,O., Tan,C.P., Naslund,T.I., Liljestrom,P., Weber,F. and Reis e Sousa,C. (2006) RIG-I-mediated antiviral responses to single-stranded RNA bearing 5′-phosphates. *Science*, **314**, 997–1001.
8. Frazier,K.S. (2015) Antisense oligonucleotide therapies: the promise and the challenges from a toxicologic pathologist's perspective. *Toxicol. Pathol.*, **43**, 78–89.
9. Kariko,K., Buckstein,M., Ni,H. and Weissman,D. (2005) Suppression of RNA recognition by Toll-like receptors: the impact of nucleoside modification and the evolutionary origin of RNA. *Immunity*, **23**, 165–175.
10. Robbins,M., Judge,A., Liang,L., McClintock,K., Yaworski,E. and MacLachlan,I. (2007) 2′-O-methyl-modified RNAs act as TLR7 antagonists. *Mol. Ther.*, **15**, 1663–1669.
11. Hamm,S., Latz,E., Hangel,D., Muller,T., Yu,P., Golenbock,D., Sparwasser,T., Wagner,H. and Bauer,S. (2010) Alternating 2′-O-ribose methylation is a universal approach for generating non-stimulatory siRNA by acting as TLR7 antagonist. *Immunobiology*, **215**, 559–569.
12. Sarvestani,S.T., Stunden,H.J., Behlke,M.A., Forster,S.C., McCoy,C.E., Tate,M.D., Ferrand,J., Lennox,K.A., Latz,E., Williams,B.R. *et al.* (2015) Sequence-dependent off-target inhibition of TLR7/8 sensing by synthetic microRNA inhibitors. *Nucleic Acids Res.*, **43**, 1177–1188.
13. Gursel,I., Gursel,M., Yamada,H., Ishii,K.J., Takeshita,F. and Klinman,D.M. (2003) Repetitive elements in mammalian telomeres suppress bacterial DNA-induced immune activation. *J. Immunol.*, **171**, 1393–1400.
14. Beignon,A.S., McKenna,K., Skoberne,M., Manches,O., DaSilva,I., Kavanagh,D.G., Larsson,M., Gorelick,R.J., Lifson,J.D. and Bhardwaj,N. (2005) Endocytosis of HIV-1 activates plasmacytoid dendritic cells via Toll-like receptor-viral RNA interactions. *J. Clin. Invest.*, **115**, 3265–3275.
15. Kaminski,J.J., Schattgen,S.A., Tzeng,T.C., Bode,C., Klinman,D.M. and Fitzgerald,K.A. (2013) Synthetic oligodeoxynucleotides containing suppressive TTAGGG motifs inhibit AIM2 inflammasome activation. *J. Immunol.*, **191**, 3876–3883.
16. Steinhagen,F., Zillinger,T., Peukert,K., Fox,M., Thudium,M., Barchet,W., Putensen,C., Klinman,D., Latz,E. and Bode,C. (2018) Suppressive oligodeoxynucleotides containing TTAGGG motifs inhibit cGAS activation in human monocytes. *Eur. J. Immunol.*, **48**, 605–611.
17. Bayik,D., Gursel,I. and Klinman,D.M. (2016) Structure, mechanism and therapeutic utility of immunosuppressive oligonucleotides. *Pharmacol. Res.*, **105**, 216–225.
18. Gantier,M.P. and Williams,B.R. (2010) Monitoring innate immune recruitment by siRNAs in mammalian cells. *Methods Mol. Biol.*, **623**, 21–33.
19. Schmid-Burgk,J.L., Schmidt,T., Gaidt,M.M., Pelka,K., Latz,E., Ebert,T.S. and Hornung,V. (2014) OutKnocker: a web tool for rapid and simple genotyping of designer nuclease edited cell lines. *Genome Res.*, **24**, 1719–1723.
20. Pelka,K., Phulphagar,K., Zimmermann,J., Stahl,R., Schmid-Burgk,J.L., Schmidt,T., Spille,J.H., Labzin,L.I., Agrawal,S., Kandimalla,E.R. *et al.* (2014) Cutting edge: the UNC93B1 tyrosine-based motif regulates trafficking and TLR responses via separate mechanisms. *J. Immunol.*, **193**, 3257–3261.
21. Pepin,G., De Nardo,D., Rootes,C.L., Ullah,T.R., Al-Asmari,S.S., Balka,K.R., Li,H.M., Quinn,K.M., Moghaddas,F., Chappaz,S. *et al.* (2020) Connexin-Dependent transfer of cGAMP to phagocytes modulates antiviral responses. *mBio*, **11**, e03187-19.
22. Gantier,M.P. (2013) Strategies for designing and validating immunostimulatory siRNAs. *Methods Mol. Biol.*, **942**, 179–191.
23. Wang,X., Spandidos,A., Wang,H. and Seed,B. (2012) PrimerBank: a PCR primer database for quantitative gene expression analysis, 2012 update. *Nucleic Acids Res.*, **40**, D1144–D1149.
24. Gorden,K.K., Qiu,X., Battiste,J.J., Wightman,P.P., Vasilakos,J.P. and Alkan,S.S. (2006) Oligodeoxynucleotides differentially modulate activation of TLR7 and TLR8 by imidazoquinolines. *J. Immunol.*, **177**, 8164–8170.
25. Jurk,M., Kritzler,A., Schulte,B., Tluk,S., Schetter,C., Krieg,A.M. and Vollmer,J. (2006) Modulating responsiveness of human TLR7 and 8 to small molecule ligands with T-rich phosphorothiate oligodeoxynucleotides. *Eur. J. Immunol.*, **36**, 1815–1826.
26. Gantier,M.P., Tong,S., Behlke,M.A., Xu,D., Phipps,S., Foster,P.S. and Williams,B.R. (2008) TLR7 is involved in sequence-specific sensing of single-stranded RNAs in human macrophages. *J. Immunol.*, **180**, 2117–2124.
27. Bailey,T.L. and Elkan,C. (1994) Fitting a mixture model by expectation maximization to discover motifs in biopolymers. *Proc. Int. Conf. Intell. Syst. Mol. Biol.*, **2**, 28–36.
28. Chow,K.T., Wilkins,C., Narita,M., Green,R., Knoll,M., Loo,Y.M. and Gale,M. Jr (2018) Differential and overlapping immune programs regulated by IRF3 and IRF5 in plasmacytoid dendritic cells. *J. Immunol.*, **201**, 3036–3050.
29. Schafer,S.L., Lin,R., Moore,P.A., Hiscott,J. and Pitha,P.M. (1998) Regulation of type I interferon gene expression by interferon regulatory factor-3. *J. Biol. Chem.*, **273**, 2714–2720.
30. Broomfield,S.A., van der Most,R.G., Prosser,A.C., Mahendran,S., Tovey,M.G., Smyth,M.J., Robinson,B.W. and Currie,A.J. (2009) Locally administered TLR7 agonists drive systemic antitumor immune responses that are enhanced by anti-CD40 immunotherapy. *J. Immunol.*, **182**, 5217–5224.
31. Chi,H., Li,C., Zhao,F.S., Zhang,L., Ng,T.B., Jin,G. and Sha,O. (2017) Anti-tumor activity of Toll-Like receptor 7 agonists. *Front. Pharmacol.*, **8**, 304.
32. Gorski,K.S., Waller,E.L., Bjornton-Severson,J., Hanten,J.A., Riter,C.L., Kieper,W.C., Gorden,K.B., Miller,J.S., Vasilakos,J.P., Tomai,M.A. *et al.* (2006) Distinct indirect pathways govern human NK-cell activation by TLR-7 and TLR-8 agonists. *Int. Immunol.*, **18**, 1115–1126.
33. Mullins,S.R., Vasilakos,J.P., Deschler,K., Grigsby,I., Gillis,P., John,J., Elder,M.J., Swales,J., Timosenko,E., Cooper,Z. *et al.* (2019) Intratumoral immunotherapy with TLR7/8 agonist MEDI9197 modulates the tumor microenvironment leading to enhanced activity when combined with other immunotherapies. *J. Immunother. Cancer*, **7**, 244.
34. Heil,F., Hemmi,H., Hochrein,H., Ampenberger,F., Kirschning,C., Akira,S., Lipford,G., Wagner,H. and Bauer,S. (2004) Species-specific recognition of single-stranded RNA via toll-like receptor 7 and 8. *Science*, **303**, 1526–1529.
35. Pockros,P.J., Guyader,D., Patton,H., Tong,M.J., Wright,T., McHutchison,J.G. and Meng,T.C. (2007) Oral resiquimod in chronic HCV infection: safety and efficacy in 2 placebo-controlled, double-blind phase IIa studies. *J. Hepatol.*, **47**, 174–182.
36. Dudek,A.Z., Yunis,C., Harrison,L.I., Kumar,S., Hawkinson,R., Cooley,S., Vasilakos,J.P., Gorski,K.S. and Miller,J.S. (2007) First in human phase I trial of 852A, a novel systemic toll-like receptor 7 agonist, to activate innate immune responses in patients with advanced cancer. *Clin. Cancer Res.*, **13**, 7119–7125.
37. Tanji,H., Ohto,U., Shibata,T., Taoka,M., Yamauchi,Y., Isobe,T., Miyake,K. and Shimizu,T. (2015) Toll-like receptor 8 senses degradation products of single-stranded RNA. *Nat. Struct. Mol. Biol.*, **22**, 109–115.
38. Crooke,S.T., Wang,S., Vickers,T.A., Shen,W. and Liang,X.H. (2017) Cellular uptake and trafficking of antisense oligonucleotides. *Nat. Biotechnol.*, **35**, 230–237.

39. Pepin,G., Ferrand,J. and Gantier,M.P. (2017) Assessing the Off-Target effects of miRNA inhibitors on innate immune Toll-Like receptors. *Methods Mol. Biol.*, **1517**, 127–135.
40. Kortylewski,M., Swiderski,P., Herrmann,A., Wang,L., Kowolik,C., Kujawski,M., Lee,H., Scuto,A., Liu,Y., Yang,C. *et al.* (2009) In vivo delivery of siRNA to immune cells by conjugation to a TLR9 agonist enhances antitumor immune responses. *Nat. Biotechnol.*, **27**, 925–932.
41. Poeck,H., Besch,R., Maihoefer,C., Renn,M., Tormo,D., Morskaya,S.S., Kirschnek,S., Gaffal,E., Landsberg,J., Hellmuth,J. *et al.* (2008) 5′-Triphosphate-siRNA: turning gene silencing and Rig-I activation against melanoma. *Nat. Med.*, **14**, 1256–1263.
42. Gantier,M.P., Tong,S., Behlke,M.A., Irving,A.T., Lappas,M., Nilsson,U.W., Latz,E., McMillan,N.A. and Williams,B.R. (2010) Rational design of immunostimulatory siRNAs. *Mol. Ther.*, **18**, 785–795.
43. Moreira,D., Adamus,T., Zhao,X., Su,Y.L., Zhang,Z., White,S.V., Swiderski,P., Lu,X., DePinho,R.A., Pal,S.K. *et al.* (2018) STAT3 inhibition combined with CpG immunostimulation activates antitumor immunity to eradicate genetically distinct Castration-Resistant prostate cancers. *Clin. Cancer Res.*, **24**, 5948–5962.
44. Barrat,F.J., Meeker,T., Gregorio,J., Chan,J.H., Uematsu,S., Akira,S., Chang,B., Duramad,O. and Coffman,R.L. (2005) Nucleic acids of mammalian origin can act as endogenous ligands for Toll-like receptors and may promote systemic lupus erythematosus. *J. Exp. Med.*, **202**, 1131–1139.
45. Hassler,M.R., Turanov,A.A., Alterman,J.F., Haraszti,R.A., Coles,A.H., Osborn,M.F., Echeverria,D., Nikan,M., Salomon,W.E., Roux,L. *et al.* (2018) Comparison of partially and fully chemically-modified siRNA in conjugate-mediated delivery in vivo. *Nucleic Acids Res.*, **46**, 2185–2196.
46. Skold,A.E., Hasan,M., Vargas,L., Saidi,H., Bosquet,N., Le Grand,R., Smith,C.I. and Spetz,A.L. (2012) Single-stranded DNA oligonucleotides inhibit TLR3-mediated responses in human monocyte-derived dendritic cells and in vivo in cynomolgus macaques. *Blood*, **120**, 768–777.